International Journal of Thermofluid Science and Technology (2023)
Volume 10, Issue 1, Paper No. 100102
https://doi.org/10.36963/IJTST.2023100102
Research Article

Onset of double diffusive surface-tension driven convection in fluid layer overlying a layer of anisotropic porous layer with soret effect

Gangadharaiah Y H

Department of Mathematics, RV Institute of Technology and Management, Bangalore, India

ARTICLE INFO

Received: 07 Dec. 2022;
Received in revised form:
15 Feb. 2023;
Accepted: 18 Feb. 2022;
Published online:
20 Feb. 2022

Keywords:
composite layer
mechanical anisotropy
thermal anisotropy
soret parameter.

ABSTRACT

The onset of double-diffusive surface tension-driven convective motion in a fluid layer overlying a fluid-saturated anisotropic porous layer is investigated analytically in the presence of the soret effect. We considered boundaries to be insulating to temperature perturbations. The governing equation that satisfies the composite system is analyzed by the normal mode approach and solved by the regular perturbation technique for linear stability. By solving coupled equations, a mathematical expression for the critical Marangoni number is obtained. Under the effect of the anisotropy, soret parameters and the impact of various physical parameters on the start of convective motion is illustrated graphically, and the stability system is investigated.

1. Introduction

Convective instability in a two-layer system, caused by temperature/concentration gradients and associated with buoyancy/surface-driven force, occurs in a variety of natural and engineering applications, including geothermal structures, electronic component chilling, defense and space, underground nuclear waste containment, petroleum extraction, groundwater contamination, heat exchangers, and chemical production (Vafai [1]; Nield and Bejan [2] ; Nield and Bejan [3]; Chen [4] ; Khalili [5] ; Suma et al.[6]; Gangadharaiah[7]; Shivakumara et al.[8]; Shivakumara et al.[9]; Gangadharaiah[10]).

Marangoni convection is convection caused by a surface tension gradient. Even slight changes in temperature or solute concentration can result in convection since surface tension on the free surface is a large function of both those variables. The thermal diffusion process, commonly known as the Soret effect, is induced by a temperature gradient. Heating the fluid layer on top of a porous bed that is saturated with fluid exhibits a number of properties that differ from convective motion in a one-layer system with or without a gravity field(Chen and Chen[11] ; Chen and Chen[12]; Chen and Chen[13]; Kolchanova et al.[14]; Chen and Hsu [15]; Si-Cheng et al.[16]; Kolchanova and Kolchanov [17]).

Corresponding e-mail: gangu.honnappa@gmail.com (Gangadharaiah Y H)

NOMENCLATURE

a	horizontal wave number	Ms	solute Marangoni number
D	differential operator d/dz	M_c	critical Marangoni number
η	thermal anisotropic parameter	p	pressure
k_C	solutal diffusivity	k_T	thermal diffusivity
W	perturbed vertical velocity	T	temperature
Da	Darcy number	ξ	mechanical anisotropic parameter
ζ	depth ratio	$\vec{V}$	velocity vector (u, v, w)
∇_h^2	horizontal Laplacian operator	α_T	coefficient of thermal expansion
∇^2	Laplacian operator	C	concentration
Pr	Prandtl number	Le	Lewis number
Sr	soret parameter	θ	amplitude of perturbed temperature

Convective motion can be induced as short-wave rolls in the liquid layer overlaying a porous matrix depending on the layer parameters (layer thickness ratios, thermal conductivity ratios, Darcy number, etc.). In this case, the fluid balancing in the layers displays bimodal neutral stability curves. Convection was explored experimentally in a 4 cm thick layer of aqueous glycerin mixture partially packed with 3 mm glass balls (see Chen and Chen[12]). The balls separated the layer into two portions, one porous and the other non-porous. After the system's equilibrium stability was lost, the creation of convective structures was seen. The depth ratio, which ranged from 0.1 to 0.2, resulted in an eightfold shrinkage in their wavelength.

Platten and Chavepeyer [18] presented the Schmidt-Milverton plots for the solutal convection issue for water-methanol and water-isopropanol by considering the composite system. They have demonstrated that expected values and theoretical values are consistent throughout the period. Gangadharaiah [19] examined double-diffusive surface-driven convective motion in a two-layer system by using the regular perturbation approach to solve the associated Eigenvalue problem. Sumithra and Komala [20] studied the impact of temperature gradients on the beginning of solutal convective motion in a composite configuration with a free upper surface and a stiff lower boundary. Hussam K. Jawad [21] looked at natural convective motion and the thermo-diffusion effect in a composite-layered system. They discovered that a positive thermo-diffusion parameter implies that the denser component travels towards the cooler side of the system, whereas a negative sign suggests that the less dense component flows towards the colder side. The salt finger's convective motion in a composite layer with stiff boundaries was examined by Komala and Sumithra [22]. Gangadharaiah [23] studied salt finger's surface-driven convection in a fluid-porous system. Internal heating effects on double-diffusive convection in a fluid atop a porous layer were studied by Gangadharaiah et al. [24]. They used the regular perturbation approach to solve the resulting Eigenvalue problem and discovered that increasing the internal heat sources in both layers can stabilize the system. An investigation on double-diffusive Marangoni convection in the composite binary fluid may be used to solidify binary solutions or alloys in a gravitational field(Chen[25], Gangadharaiah and Suma[26], Chen et al.[27], Gangadharaiah[28], Tait and Jaupart[29], Gangadharaiah[30], Worster[31] Gangadharaiah and Anand[32] and Gangadharaiah [33]). A directed upward concentration gradient of a solution's heavier component arises when it is cooled and solidified from below. The increase of shortwave perturbations of the immobile state causes convective fluid flows in a solution layer overlaying a porous bed (mushy zone) that arises towards the upper crystal boundary (Worster[31]). A crystal is deformed by convection in the solution and nearby mushy zone. The development of double-diffusive fingers towards the top edge of the mushy zone is caused by short-wave instability. In this study, the impact of the soret parameter on the salt finger's convective motion in a fluid layer overlying an anisotropic porous layer is analyzed analytically and the results are discussed graphically.

2. Conceptual Model

The system under investigation consists of a fluid layer of thickness d (region1) and saturating an underlying anisotropic porous layer of thickness d_m (region2) under zero gravity. Thus the z indicating distances are vertically upward. The fluid-porous interface at $z=0$. The surface tension σ is assumed to vary linearly with temperature in the form $\sigma=\sigma_0-\sigma_T\left(T-T_0\right)$, where σ_0 is the unperturbed value and $-\sigma_T$ is the rate of change of surface tension with temperature.

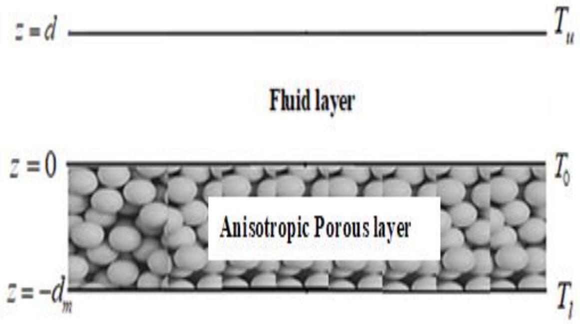

Fig. 1 Physical configuration

3. Mathematical Formulation

For the proposed scheme, the governing equations are:

Region1: fluid layer $\left(0\le z\le d\right)$

$$\nabla\cdot\vec{V}=0 \quad (1)$$

$$\rho_0\left[\frac{\partial\vec{V}}{\partial t}+\left(\vec{V}\cdot\nabla\right)\vec{V}\right]=-\nabla p+\mu\nabla^2\vec{V} \quad (2)$$

$$\frac{\partial T}{\partial t}+\left(\vec{V}\cdot\nabla\right)T=\kappa\nabla^2 T \quad (3)$$

$$\frac{\partial C}{\partial t}+\left(\vec{V}\cdot\nabla\right)C=\kappa_c\nabla^2 C+\kappa_T\nabla^2 T \quad (4)$$

Region2: porous layer $\left(-d_m\le z\le 0\right)$

$$\nabla\cdot\vec{V}_m=0 \quad (5)$$

$$\frac{\rho_0}{\phi}\frac{\partial\vec{V}_m}{\partial t}=-\nabla p_m-\mu\underset{\sim}{K}^{-1}\cdot\vec{V}_m \quad (6)$$

$$A\frac{\partial T_m}{\partial t}+\left(\vec{V}_m\cdot\nabla_m\right)T_m=\nabla\cdot\left\{\underset{\sim}{\kappa}_m\cdot\nabla T_m\right\} \quad (7)$$

$$\phi\frac{\partial C_m}{\partial t}+\left(\vec{V}_m\cdot\nabla_m\right)C_m=\kappa_{Cm}\nabla^2 C_m+\kappa_{Tm}\nabla^2 T_m \quad (8)$$

The effective thermal diffusivity and tensors of permeability are given by $\underset{\sim}{\kappa}_m=\kappa_{mh}(\hat{i}\hat{i}+\hat{j}\hat{j})+\kappa_{mv}\hat{k}\hat{k},\ \underset{\sim}{K}=K_h(\hat{i}\hat{i}+\hat{j}\hat{j})+K_v\hat{k}\hat{k}.$

After linearizing Equations (1)–(8), the variables are nondimensionalized using $\frac{\kappa}{d},\frac{d^2}{\kappa},T_0-T_u$ and C_0-C_u as the nondimensional variables of velocity, time, temperature and concentration in region-1 and $\frac{\kappa_m}{d_m},\frac{d_m^2}{\kappa},T_l-T_0$ and C_l-C_0 as the associated nondimensional variables in region-2. For the perturbed variables, the dimensionless equations are as follows:

For region-1,

$$\left[\frac{1}{pr}\frac{\partial}{\partial t}-\nabla^2\right]\nabla^2 w=0 \quad (9)$$

$$\left(\frac{\partial}{\partial t}-\nabla^2\right)T=w \quad (10)$$

$$\frac{\partial C}{\partial t}=w+\frac{1}{Le}\nabla_h^2 C \quad (11)$$

For region-2,

$$\left[\frac{Da}{Pr_m}\frac{\partial}{\partial t}+\xi\nabla_{mh}^2+\frac{\partial^2}{\partial z_m^2}\right]w_m=0 \quad (12)$$

$$\left(A\frac{\partial}{\partial t}-\frac{\partial^2}{\partial z_m^2}-\eta\nabla_{mh}^2\right)T_m=w \quad (13)$$

$$\phi\frac{\partial C_m}{\partial t}=w_m+\frac{1}{Le}\nabla_{hm}^2 C_m \quad (14)$$

Here, $Pr=\nu/\kappa$, $Le=\frac{k}{k_c}$, $\nabla^2=\nabla_h^2+\partial^2/\partial z^2$, $\nabla_h^2=\partial^2/\partial x^2+\partial^2/\partial y^2$, $Pr_m=\nu/\kappa_m=Pr\varepsilon_T$, $Sr=\frac{\kappa_T\Delta T}{\kappa_c\Delta C}$, $Le_m=\frac{k_m}{k_{Cm}}$, $\xi=\frac{K_x}{K_z}$, $\eta=\frac{k_{mx}}{k_{mz}}$, $\nabla_m^2=\nabla_{mh}^2+\partial^2/\partial z_m^2$, $\nabla_{mh}^2=\partial^2/\partial x_m^2+\partial^2/\partial y_m^2$ and $Da=K/d_m^2$.

In order to analyze arbitrary disturbance in terms of normal modes, we suppose that the perturbations w,T and θ have the forms

$$(w,T,C)=\{W(z),\Theta(z),\Omega(z)\}\exp\left[i(lx+my)\right] \quad (15)$$

$$(w_m,T_m,C_m)=\{W_m(z),\Theta_m(z),\Omega_m(z)\}\exp\left[i\left(\tilde{l}x+\tilde{m}y\right)\right] \quad (16)$$

and substituting them in Eqs. 9–14 (with $\frac{\partial}{\partial t}=0$), we obtain the following ordinary differential equations:

In region-1,

$$\left(D^2-a^2\right)^4 W=0 \quad (17)$$

$$\left(D^2-a^2\right)\Theta=-W \quad (18)$$

$$\left(\frac{1}{Le}\left(D^2-a^2\right)\right)\Omega+S_r\left(D^2-a^2\right)\Theta=-W \quad (19)$$

In region-2,

$$\left(\frac{1}{\xi}D_m^2-a_m^2\right)W_m=0 \quad (20)$$

$$\left(D_m^2-\eta a_m^2\right)\Theta_m=-W_m \quad (21)$$

$$\left(\frac{1}{Le_m}\left(D_m^2-a_m^2\right)\right)\Omega_m+S_{rm}\left(D_m^2-a_m^2\right)\Theta_m=-W_m \quad (22)$$

where $D=d/dz$, $a=\sqrt{l^2+m^2}$ and $a_m=\sqrt{\tilde{l}^2+\tilde{m}^2}$.

The preceding relevant boundary conditions have been used to solve these ordinary differential equations through using the regular perturbation approach, following Shivakumara et al.[8] and Komala and Sumithra[20].

4. Boundary Conditions

At $z=1$,

$$W=D\Theta=D\Omega=D^2W+M\,a^2\Theta+M_s\,a^2\Omega=0 \quad (23)$$

At $z_m=-1$,

$$W_m=D_m\Theta_m=D_m\Omega_m=0 \quad (24)$$

At $z=0$,

$$W=\frac{\zeta}{\varepsilon_T}W_m \quad (25)$$

$$\Theta=\frac{\varepsilon_T}{\zeta}\Theta_m \quad (26)$$

$$\Omega=\frac{\varepsilon_S}{\zeta}\Omega_m \quad (27)$$

$$D\Theta=D_m\Theta_m \quad (28)$$

$$D\Omega=D_m\Omega_m \quad (29)$$

$$\left[D^2-3a^2\right]DW=\frac{-\zeta^4}{Da\varepsilon_T}D_mW_m \quad (30)$$

$$\left[D^2-\frac{\beta\zeta}{\sqrt{Da}}D\right]W=\frac{-\beta\zeta^3}{\sqrt{Da}\varepsilon_T}D_mW_m \quad (31)$$

5. Method of Solution

For the steady temperature and concentration flux bounds, convection occurs at minimum value of a. That is,

$$(W,\Theta,\Omega)=\sum_{i=0}^{N}\left(a^2\right)^i\left(W_i,\Theta_i,\Omega_i\right) \quad (32)$$

$$(W_m,\Theta_m\Omega_m)=\sum_{i=0}^{N}\left(\frac{a^2}{\zeta^2}\right)^i\left(W_{mi},\Theta_{mi},\Omega_{mi}\right) \quad (33)$$

Substitution of Eqs. (32) and (33) into Eqs. $(15)-(22)$ and the boundary conditions $(23)-(31)$ and considering like powers of a^2, we get zeroth order equations whose solution are as follows

$$W_0=0,\quad \Theta_0=\frac{\varepsilon_T}{\zeta},\quad \Omega_0=\frac{\varepsilon_s}{\zeta} \quad (34)$$

$$W_{m0}=0,\quad \Theta_{m0}=1,\quad \Omega_{m0}=1 \quad (35)$$

The equations at the first order in a^2 are

For region-1,

$$D^4W_1=0 \quad (36)$$

$$D^2\Theta_1=-W_1+\frac{\varepsilon_T}{\zeta} \quad (37)$$

$$D^2\Omega_1=-Le(1-Sr)W_1+\frac{\varepsilon_s}{\zeta} \quad (38)$$

For region-2,

$$D_m^2W_{m1}=0 \quad (39)$$

$$D_m^2\Theta_{m1}=W_{m1}+1 \quad (40)$$

$$D^2\Omega_{m1}=-\left(\eta+1-Le_mSr_m\right)W_{m1}+\left(1+Le_mSr_m\right) \quad (41)$$

and the boundary conditions $(23)-(31)$ become

$$W_1=0,\ D\Theta_1=0, D\Omega_1=0\ at\quad z=1 \quad (42)$$

$$D^2W_1+M\frac{\varepsilon_T}{\zeta}+M_s\frac{\varepsilon_s}{\zeta}=0\ \ at\ z=1 \quad (43)$$

$$W_{m1}=0, D_m\Theta_{m1}=0, D_m\Omega_{m1}=0\,at\,z_m=-1 \quad (44)$$

And at the interface

$$W_1 = \frac{1}{\zeta\varepsilon_T} W_{m1} \quad (45)$$

$$\Theta_1 = \frac{\varepsilon_T}{\zeta^3}\Theta_{m1} \quad (46)$$

$$D\Theta_1 = \frac{1}{\zeta^2} D_m \Theta_{m1} \quad (47)$$

$$D\Omega_1 = \frac{1}{\zeta^2} D_m \Omega_{m1} \quad (48)$$

$$D^3 W_1 = \frac{\zeta^2}{\varepsilon_T \xi Da} D_m W_{m1} \quad (49)$$

$$D^2 W_1 - \frac{\beta\zeta}{\sqrt{\xi Da}} DW_1 = \frac{\beta\zeta}{\varepsilon_t \sqrt{\xi Da}} D_m W_{m1} \quad (50)$$

The general solutions of Eq. (36) and (39) are respectively given by

$$W_1 = \left[C_1 + C_2 z + C_3 z^2 + C_4 z^3 \right] \quad (51)$$

$$W_{m1} = \left[C_5 + C_6 z_m \right] \quad (52)$$

where

$$C_1 = \left(\frac{Sr}{\varepsilon_s \xi} - \frac{\zeta^2 Le_m}{\varepsilon_T \xi} + b_1 \right),$$

$$C_2 = \left(\frac{2Le\varepsilon_T}{\zeta^2} - \frac{C_1 M_s}{2\xi} - \frac{e^{\eta} b_2}{\zeta^2} \right), \quad C_3 = \frac{(b_3 + b_4 C_2)}{b_5},$$

$$C_4 = \frac{(b_6 \varepsilon_T \zeta - \varepsilon_s \zeta C_3)}{Sr_m \xi C_1},$$

$$C_5 = \frac{LeC_1}{2\zeta(1+2Sr)}, C_6 = \frac{(\varepsilon_T \eta - \varepsilon_s \zeta C_3)}{Sr_m \xi \eta},$$

$$b_1 = \left(\frac{2\zeta^2 Le_m \sqrt{Da}}{2\xi} + Sr_m \beta \zeta^3 \right)$$

$$b_2 = \left(\eta^2 \zeta^2 Le \sqrt{Da\xi} - \beta\zeta^3 \eta \right) - \beta\zeta^3 \left(\sqrt{Da\xi} - LeSr \right),$$

$$b_3 = \left(\Delta_2 \sqrt{Da\xi} - \frac{\beta\zeta^3}{\varepsilon_T \zeta} \right),$$

$$b_4 = \left(\frac{\varepsilon_T M_s \zeta^3}{6\eta\zeta} - \frac{\beta\zeta^3 Sr \sqrt{Da\xi}}{\varepsilon_s \zeta} \right)$$

$$b_5 = (\eta - 1) Le + \sqrt{Da\xi}, \; b_6 = Le_m \left(\frac{2\varepsilon_T}{6\eta\zeta} - \frac{\sqrt{Da\xi}}{\varepsilon_s \zeta} \right).$$

Integrating Eq. 38 and 39 between $z = 0$ and 1, and Eq. 40 and 41 between $z_m = -1$ and 0, using the relevant boundary conditions and adding the resulting equations, we obtain the following solvability condition:

$$\left\{ \begin{array}{l} \{1 + Le(1 - Sr)\} \int_0^1 W_1 \, dz + \\ \frac{(\eta + 2 - Le_m Sr_m)}{\zeta^2} \int_{-1}^0 W_{m1} \, dz \end{array} \right\} = \left\{ \frac{\varepsilon_S}{\zeta} + \frac{(\eta + \varepsilon_T + 1 + Le_m Sr_m)}{\zeta^2} \right\} \quad (53)$$

Back substituting the expressions for W_1 and W_{m1} into Eq. (53). The critical Marangoni number is expressed as the result of integrating Eq. (53), which is given by

$$M_c = \frac{\left\{ \frac{\varepsilon_S}{\zeta} + \frac{(\eta + \varepsilon_T + 1 + Le_m Sr_m)}{\zeta^2} \right\} \left(\frac{Da \, \varepsilon_T^2}{\zeta^4} \right)}{(\delta_1 C_1 + \delta_2 C_2 + \delta_3 C_3 + \delta_4 C_4 + \delta_5) + \frac{(\eta + 2 - Le_m Sr_m)}{\zeta^2} (-C_5 + \delta_6 C_6 - \delta_3 \delta_7)} \quad (54)$$

where

$$\delta_1 = \left(\frac{4M_s}{Le} + 1 \right), \quad \delta_2 = \left[\frac{2Le_m}{\eta^2} + \frac{2Sr_m}{\zeta^3} + M_S \right]$$

$$\delta_3 = \left[\frac{2M_S}{3\xi} + \left(\frac{Sr}{\xi} - \frac{2Le_m}{\eta^2} + \frac{2Sr_m}{\zeta^3} \right) \right]$$

$$\delta_4 = \left[\frac{2Le}{\eta Le_m} + \zeta\eta \frac{(M_S + \eta Le_m)}{(\xi + \eta)} \right]$$

$$\delta_5 = \left[\frac{2Ms}{Le} + \left(\frac{Sr\eta}{Le} - \frac{\beta\zeta}{Sr_m Le^2} \right) \right]$$

$$\delta_6 = \left[\frac{Sr_m Ms}{Le_m} + \left(\frac{Sr}{Le_m} - \frac{\beta\zeta}{Le_m^2} \right) \right]$$

$$\delta_7 = \left[\frac{2Le}{3Sr_m} + \frac{\zeta}{Le_m} + \frac{\eta^2}{Le_m^2} + \frac{2\zeta^2}{Le_m^3} \right].$$

6. Results and Discussion

In the present work, the impact of soret parameter on the surface-driven convective motion in a composite layer is analyzed using a linear stability approach. The normal mode method is used to apply the linear analysis. The regular perturbation approach is used to tackle the eigenvalue problems derived from linear stability analyses. After addressing the current problem in which the solute is missing, the analytical results are verified (see Table 1). The current findings exhibit outstanding accordance with the outcomes determined by Shivakumara et al. [9] . The main analytical results that will be depicted below are obtained for a composite system with the following fixed parameters: $\phi =$ 0.389, Darcy number $\sqrt{Da} = 3.04\times10^{-3}$, soret parameters $Sr = 0.75, Sr_m = 0.25$, solute Marangoni number $Ms = 10$ and Lewis numbers $Le = 0.3$, $Lem = 0.2$.

Figure 2 shows how the critical Marangoni number varies against the depth ratio ζ for various values of Darcy number Da . It is evident that a lowering in Da would result in an increase in the critical Marangoni number M_c and as a result, it has the effect of delaying convective motion. For small values of depth ratio, the M_c reaches maximum. The curves of for various Da coalesce for greater values of M_c, on the other hand.

The influence of anisotropy parameters on the beginning of soret-driven convective motion is illustrated in Figs. 3 and 4, which show the fluctuation across a range of mechanical anisotropy and thermal anisotropy parameters. As shown in the graphs, M_c rise as the value of ξ decreases. This is due to the fact that a drop in n correlates to a lower horizontal permeability, which impedes fluid transport in horizontal movement. Consequently, the region-2 conduction process destabilization is quite low. And for higher values of ζ, has a more destabilizing effect.

The influence of mass diffusivity and thermal diffusivity of both fluid and porous layers on the convective motion is portrayed in Fig. 7. It is clear that an increase in Le and Lem is to enhance the Eigen function M_c and as a result, it has the effect of hastening the beginning of convection. For small values of ζ, M_c has significant effect. At higher values

becomes more steady, necessitating larger values of M_c for convection to begin. It can be seen in Fig. 4 that for a constant value of ξ, M_c, reduces as lowers. This is due to the fact that when the horizontal thermal diffusivity diminishes, so does the vertical thermal diffusivity. The inability of heat to pass through the porous layer causes the fluid's horizontal temperature variations, which are required to maintain convection, to dissipate more inefficiently for small η.

The influence of soret parameters $Sr \,\&\, Sr_m$ on M_c is plotted against the depth ratio ζ in Fig5. We observe that M_c of the insulating case is always less than that of the conducting case for each of the other parameters' potential values. Thus the effects of soret parameters make the composite system stable.

The influence of the solutal Marangoni number M_s on M_c with different values of ζ is presented in Figs. 6. It's worth noting that when the value of M_s increases, the M_c lowers. As a result, this component has a destabilizing effect, however, the rate of destabilization is quite low. And for higher values of ζ, has a more destabilizing effect

of ζ, the curves, on the other hand of M_c for different Le and Lem decreases. Figure 8 shows the vertical velocity verses eigenfunctions W and W_m for various values of Sr and Sr_m with $\eta = 0.5 = \xi$, $\zeta = 1$, and $Da = 0.003$. The existence of Sr_m has no effect on W_m, however the presence of $Sr = 2$ in the fluid layer accelerates W more than the lack of Sr in the fluid layer.

Table1 Comparison of M_c and ζ with Da when η = 0.5= ξ, ε_T = 0.725, β = 1 and $M_S = 0$

ζ	$Da = 0.001$		$Da = 0.003$		$Da = 0.005$	
	Present study	Shivakumara et al.[9]	Present study	Shivakumara et al.[9]	Present study	Shivakumara et al.[9]
0.1	5.178	5.178	3.198	3.198	2.631	2.631
0.5	68.934	68.934	42.717	42.717	31.999	31.999
1.0	72.414	72.414	64.118	64.118	58.314	58.314
1.5	66.136	66.136	62.651	62.651	60.069	60.069
2.0	62.091	62.091	60.058	60.058	58.567	58.567
2.5	59.465	59.465	58.055	58.055	57.038	57.038

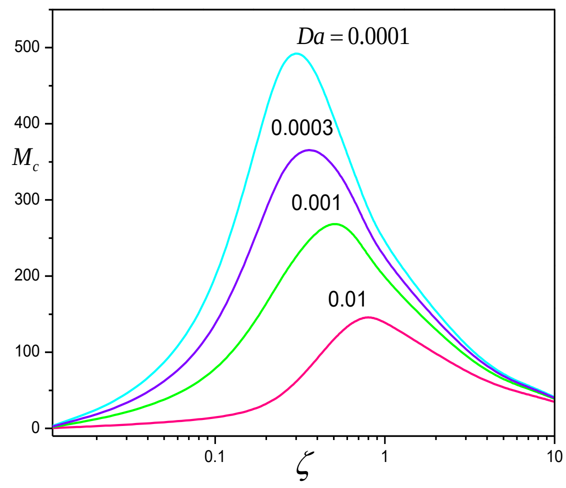

Fig. 2. Variation of M_c versus depth ratio ζ

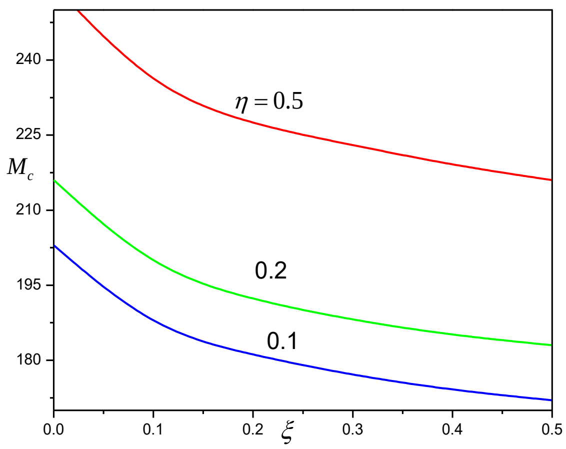

Fig. 3. Variation of M_c versus mechanical anisotropic parameter ξ

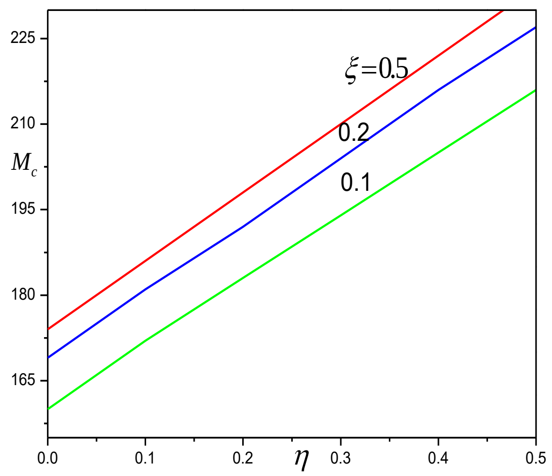

Fig. 4. Variation of M_c versus thermal anisotropic parameter η

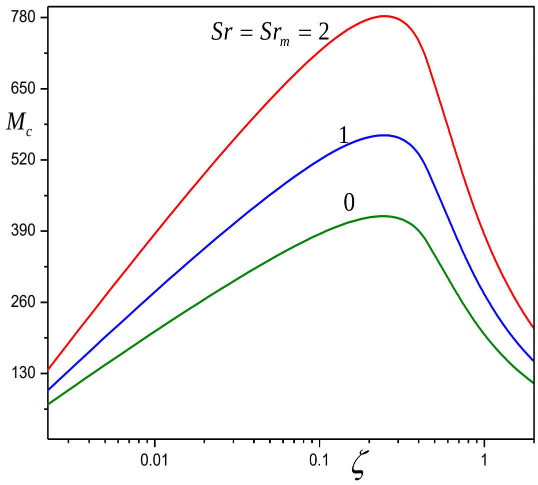

Fig. 5. Variation of M_c versus depth ratio ζ

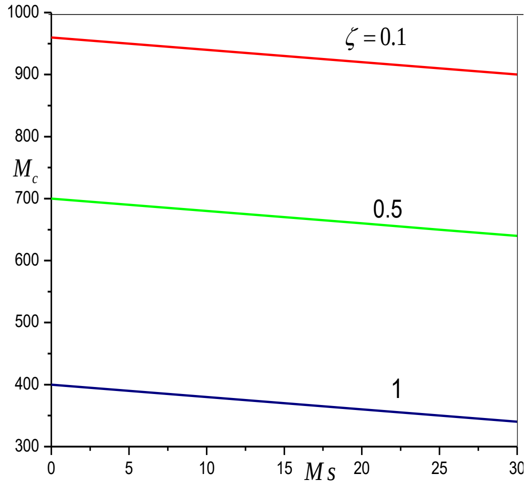

Fig. 6. Variation of M_c versus solute Marangoni number Ms

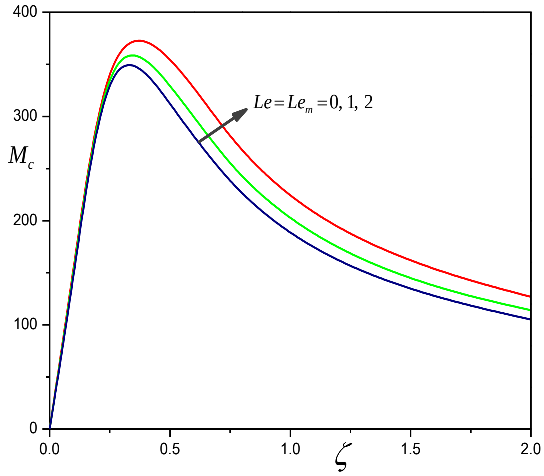

Fig. 7. Variation of M_c versus depth ratio ζ

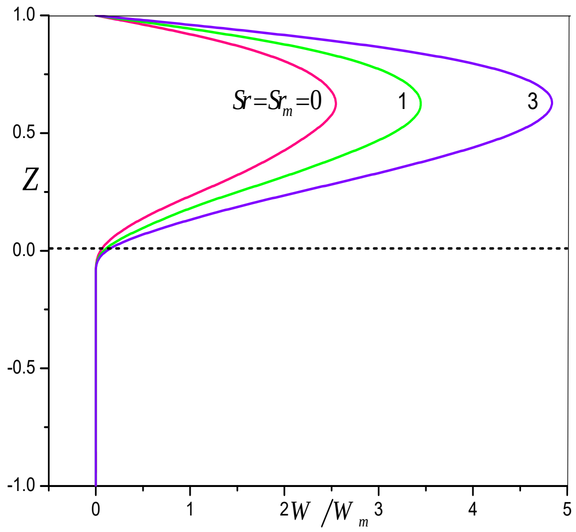

Fig. 8. perturbed vertical velocity versus eigenfunctions with $\zeta=1$ and fixed value of other parameters.

7. Conclusions

The double-diffusive soret-driven convective motion in a fluid layer overlying an anisotropic porous matrix is studied using linear stability analysis. The following are the key conclusions of the linear stability analysis:

• The influence of a rising Lewis number, soret parameters, and thermal anisotropic parameters are found to delay the onset of convective motion, while solute Marangoni number, porous parameter, and mechanical anisotropic parameters are adjusted to increase the beginning convective motion.

• With increasing Darcy number, solute Marangoni number, and mechanical anisotropic parameter, the size of convective cells decreases, however, depth ratio has a dual nature on the dimension of convective cells.

• The depth ratio plays a crucial role in the control of the soret-driven convective motion in the composite system.

References

[1] K. Vafai. Handbook of Porous Media Taylor/CRC Press, Francis, London/Boca Raton, FL, 2005
[2] Nield D.A., and A. Bejan, Convection in Porous Media. Springer, Berlin,2006.
[3] Nield D.A., and A. Bejan, Convection in Porous Media . Springer, New York,2013.
[4] Chen, F, Throughflow effects on convective instability in superposed fluid and porous Layers, J. Fluid. Mech, 231,(1990) 113–133.
[5] Khalili A, Shivakumara I.S, Suma, S.P, Convective instability in superposed fluid and porous layers with vertical throughflow,Transp. Porous Med,51(2003) 1–18.
[6] Suma S.P, Gangadharaiah Y.H, Indira R., Shivakumara I.S,Throughflow effects on penetrative convection in superposed fluid and porous layers, Transp. Porous Med,95(2012) 91-110.
[7] YH Gangadharaiah, Double diffusive Marangoni convection in superposed fluid and porous layers, Int. J. Innovative Research Sci. Eng. Tech,2(2013) 2625-2633.
[8] Shivakumara I.S, Suma S.P, Indira R, Gangadharaiah Y.H, Effect of internal heat generation on the onset of Marangoni convection in a fluid layer overlying a layer of an anisotropic porous medium, Transp. Porous Med,92(2012) 727–743.
[9] Shivakumara, I. S, Jinho Lee. and Chavaraddi K. B, Onset surface tension convection in a fluid layer overlying a layer of an anisotropic porous medium, Int. J. Heat Mass Transf,53(2011) 994-1001.
[10] Gangadharaiah Y.H, Onset of Benard–Marangoni convection in a composite layer with an anisotropic porous material, Journal of Applied Fluid Mechanics,9(2016)1551-1558.
[11] F. Chen, C. Chen,Onset of finger convection in a horizontal porous layer underlying a fluid layer, ASME J. Heat Transfer,110(1998)403–409.
[12] F. Chen, C. Chen, Experimental investigation of convective stability in a superposed fluid and porous layer when heated from below, J. Fluid Mech,20(1989)311–321.
[13] F. Chen, C. Chen,. Convection in superposed fluid and porous layers,.J. Fluid Mech,234(1992)97–119.
[14] E. Kolchanova, D. Lyubimov, T. Lyubimova,The onset and nonlinear regimes of convection in a two-layer system of fluid and porous medium saturated by the fluid, Transport Porous Media,97(2013)25–42.
[15] F. Chen, L. Hsu, Onset of thermal convection in an anisotropic and inhomogeneous porous layer underlying a fluid layer,J. Appl. Phys,69(1991)6289.
[16] Z. Si-Cheng, L. Qiu-Sheng, N. Henri, B. Bernard, Gravity-driven instability in a liquid

Corresponding e-mail: gangu.honnappa@gmail.com (Gangadharaiah Y H)

film overlying an inhomogeneous porous

[17] E. Kolchanova, N. Kolchanov,Nonlinear convection regimes in a fluid layer partially filled with an inhomogeneous porous medium, Bull. Perm Univ. (Phys.),37(2017) 22–30.

[18]J. K. Platten and G. Chavepeyer,Oscillatory motion in Bénard cell due to the Soret effect,Journal of Fluid Mechanics,60(1973) 305 - 319

[19] Y.H. Gangadharaiah,Double diffusive surface-driven convection in a fluid- porous system. International Journal of Thermofluid Science and Technology,8(2021) 080301.

[20]Sumithra R, Komal and Manjunatha,Darcy-Benard double-diffusive Marangoni convection with soret effect in a composite system , Malaya J Mat,8(2020)1473-1479.

[21] Jawad, Hussam K,Natural convection and soret effect in a multi-layered liquid and porous system. Theses and dissertations,2022;1512.

[22] Komal and Sumithra R, Effects of uniform and non-uniform salinity gradients on the onset of double-diffusive convection in a composite layer: an analytical study,ARPN J Eng Appl Sci,14(2019)856-868.

[23] YH Gangadharaiah,Double diffusive Marangoni convection in superposed fluid and porous layers, Int. J. Innovative Research Sci. Eng. Tech,2(2013) 2625-2633.

[24] Y.H. Gangadharaiah, S. P. Suma, Nagarathnamma H and T. Y. Chaya, Double-diffusive penetrative convection in a fluid overlying a porous layer,International Journal of Thermofluid Science and Technology,9(2022) 090103.

[25] C. Chen, F. Chen, Experimental study of directional solidification of aqueous ammonium chloride solution, J. Fluid Mech, 227 (1991) 567–586.

layer,Chin. Phys. Lett,28(2011)024702.

[26] Gangadharaiah, Y. H., Suma, S. P., Bernard-Marangoni convection in a fluid layer overlying a layer of an anisotropic porous layer with a deformable free surface, Advanced Porous Materials, 1(2), (2013)229-238.

[27] F. Chen, J. Lu, T. Yang, Convective instability in ammonium chloride solution directionally solidified from below, J. Fluid Mech, 276 (1994) 163–187.

[28] Gangadharaiah, Y. H., Influence of Throughflow Effects Combined with Internal Heating on the Onset of Convection in a Fluid Layer Overlying an Anisotropic Porous Layer, Journal of Advanced Mathematics and Applications,6 (2017)79-86.

[29] S. Tait, C. Jaupart, Compositional convection in a reactive crystalline mush and melt differentiation, J. Geophys. Res, 97 (1992) 6735–6756.

[30] Gangadharaiah, Y. H., Effects of Internal Heat Generation and Variable Viscosity on Marangoni Convection in Superposed Fluid and Porous Layers, Journal of Advanced Mathematics and Applications,3 (2014)158-164.

[31] M. Worster, Instabilities of the liquid and mushy regions during solidification of alloys, J. Fluid Mech, 237 (1992) 649–669.

[32] Gangadharaiah YH and Ananda K, Influence of viscosity variation on surface driven convection in a composite layer with a boundary slab of finite thickness and finite thermal conductivity, JP Journal of Heat and Mass Transfer.19(2020)269-288.

[33] Y.H. Gangadharaiah, Onset of surface driven convection in self-rewetting fluid layer overlying a porous medium. International Journal of Thermofluid Science and Technology,9(2022) 090504.